

# Nano Indentation Comparison Of Cartilage, Bone And A Poly Trimethylene Carbonate Composite

Rahul Ribeiro\*

\*Department of Mechanical Engineering, Padre Conceição College of Engineering, Verna, Goa, India, 403722.

## ABSTRACT

This study investigates the comparative behaviour of cartilage, bone, UHMWPE and a Poly trimethylene carbonate PTMC composite with hydroxyapatite and carbon nanotubes (PHN), under identical nano-indentation loading-unloading. The loading was a controlled linear increasing force followed by a static force period followed by a final linear decrease to zero. The corresponding load-penetration depth curves exhibited curved increasing and decreasing behaviour as the load was increased and decreased. During the static load period, the materials exhibited creep to different extents. The penetration depth during unloading did not follow that during loading thereby exhibiting hysteresis. The average stiffness, hardness and reduced modulus were highest for cartilage and lowest for UHMWPE. Correspondingly, the depth of penetration was lowest for cartilage and highest for UHMWPE. However, the standard deviation of the values was found to be much higher for the natural materials cartilage and bone as compared to UHMWPE and PHN, indicating a complex hierarchical structure of the tissues. The behaviour of PHN was closer to that of the natural tissues as compared to the behavior of UHMWPE.

**Keywords-** Nano indentation, biomaterials, biomechanics, composite

**How to cite this article:** Ribeiro R, Nano Indentation Comparison Of Cartilage, Bone And A Poly Trimethylene Carbonate Composite. Int J Drug Deliv Technol. 2026;16(4s): 563-572; DOI: 10.25258/ijddt.16.4s.66

## Introduction

Nanoindentation has been used as a mechanical characterization technique at sub-micron scales [1, 2, 3, 4, 5, 6, 7, 8, 9]. It provides a correlation between histological findings, disease state and mechanical behavior at the nano-level [10]. It has been found that mechanical behavior is sometimes different at the macro, micro and nano scales. Nanoindentation involves the application of a controlled load to the surface to induce local surface deformation [10]. Biological tissues and biomaterials are known to have a hierarchical structure, which can be characterized at the sub-micron level. Several authors have investigated various tissues at the nano-level using nanoindentation [11, 12, 13, 14, 15, 16, 17]. Cartilage tissue is a natural composite material having a unique molecular structure. Articular cartilage at bone joints have a non-uniform distribution of collagen fibers, proteoglycan molecules, chondrocyte cells and fluids, based on its functionality. Arthritis is a disease related to cartilage degeneration, which affect more than 350 million people and is a leading cause of disability [18]. There are several ways in which arthritis is treated, depending on its severity. Total joint replacements are a common treatment method for severe arthritis, in which cartilage and bone tissue from both sides of the joint are surgically removed and synthetic biomaterial components are inserted in their place. Several authors have investigated the possibility of replacing cartilage with synthetic biomaterials [19, 20, 21, 22, 23, 24, 25, 26, 27].

Several tissues and polymers exhibit time-dependent visco-elasticity. The compliance method can therefore give a wrong indication of the mechanical properties. Therefore, after the initial linear loading, there is a hold period to allow deformation to stabilize [28, 29].

A material suitable for integration with bone should have sufficient porosity and mechanical strength to allow cell adhesion, cell migration, growth, and proliferation<sup>30</sup>. It has been found that Hydroxyapatite (HAP) has the ability to stimulate osteoinduction and has shown good integration with bone.<sup>31, 32, 33</sup> have reported that a copolymer of polytrimethylene carbonate (PTMC) supported the highest degree of human articular cartilage chondrocyte cell adhesion. PTMC and its copolymers have been used in the medical industry as resorbable sutures<sup>34</sup> drug delivery systems<sup>35</sup> pins and screws for bone fixation<sup>36</sup> and temporary three dimensional scaffolds for tissue engineering<sup>37</sup>. Carbon nanotubes possess high tensile strength, ultralight weight, and excellent thermal and chemical stability<sup>38</sup>. Carbon-based materials have been widely used as biomaterials<sup>39, 40, 41</sup>. Carbon nanotubes are therefore a potential candidate for use as multifunctional materials in biomaterial composites. The mechanical strength can provide reinforcement similar to collagen fibers, and functionalization of the carbon nanotubes (CNT) surface can vary attractive and reactive forces within and on the surface of the composite materials. Bone mineral is primarily made up of calcium hydroxyapatite<sup>42</sup>. Furuzono et al.<sup>43</sup> studied a composite of silicone elastomer and hydroxyapatite particles. They found that the hydroxyapatite (HA) coating effectively added bioactivity to the surface.

Biomaterials are known to be complex viscoelastic composites whose mechanical performances are dependent on the multifaceted details of the internal hierarchical structure.<sup>44</sup> In this study, potential biomaterials polymer poly trimethylene carbonate combined with carbon nanotubes and hydroxyapatite,

cartilage, bone and ultra high molecular weight polyethylene (UHMWPE) were investigated using the nanoindentation method. UHMWPE was investigated for comparison, as it is a common joint replacement material. A trapezoidal loading profile was used. Mechanical properties investigated were stiffness, hardness and reduced modulus. Total penetration depth and depth due to creep were also measured and compared.

**Materials**

The materials used in this study were: monomer trimethylene carbonate (Boehringer Ingelheim, Ridgefield, CT, 1 g), Hydroxy apatite (HAP) powder (Sigma Aldrich, St. Louis, MO, 0.05 g), multi-walled carbon nanotubes (1 mg), the catalyst N,N-bis(3,5-di-tertbutylsalicylidene)-1,2-ethylenediamine Calcium (II), and the cocatalyst: N-butyl ammonium chloride [Bu<sub>4</sub>N]<sup>+</sup> Cl<sup>-</sup>.

Ring opening polymerization was conducted at 88 °C for 45 min. to synthesize PTMC, by the method of solution casting. The nanotubes and HAP were mixed in the monomer prior to polymerization. During polymerization the mixture was stirred continuously. The detailed polymerization process is described in a reference<sup>45</sup>.

The monomer:catalyst:cocatalyst molar ratio was 350:1:1. The catalyst was not removed from the final polymer as it is a calcium-based catalyst that is likely to be biofriendly and it also provides strength to the material. The synthesized polymer composite was solution cast onto flat aluminum foil cups and, on evaporation of the solvent, formed 2-mm-thick films. Because the composite contains PTMC, HAP, and carbon nanotubes (NT), we will refer to it as (PHN). UHMWPE (Goodfellow, Oakdale, PA) in processed form, was tested for comparison.

Multi-walled carbon nanotubes were obtained from Carbon Nanotechnologies Inc. Human cartilage and cancellous bone

Human articular cartilage specimen was obtained from a 51-year-old male’s amputated right knee. The patient was suffering from a vascular obstructive disease in his right leg. He had no chance of living with conservative treatment because of ischemic necrosis of the foot. His leg therefore, had to be amputated above the knee. The specimens were harvested from the joint using a hacksaw and scalpel blade. The specimens contained the entire thickness of cartilage and part of the subchondral bone. Cartilage and subchondral bone obtained from near the femoral condyle was used as the pin material in the tribological tests. Cartilage (complete thickness) and subchondral bone from the tibial plateau were used as the counter material for the cartilage–cartilage tests. Subchondral bone from the knee joint of the same subject from whom the cartilage was obtained, was used in these studies. The bone and cartilage specimens were stored in a deep freeze at -17°C. According to Collins et al<sup>46</sup>, the cartilage would have most likely undergone grade I or II osteoarthritis, based on age. All specimens were tested in dry condition, as moisture tended to interfere with the indenter tip causing erroneous readings.

**Experimental Methodology**

Nanomechanical properties were obtained using a nanoindenter (Triboindenter, Hysitron, Minneapolis, MN). The elastic, plastic, and viscoelastic behavior of tested materials surfaces can be compared over the load–time curves. The loading condition was an initial linear increase from 0 to 200N in 10s, followed by a stable load of 200N for 10s, and finally followed by a linear decrease in load from 200 to 0N over 10s (Fig 1.). Nine tests were conducted for each material for repeatability. Indents were spaced 1micrometre apart in a square matrix. Depending on the ease of deformation, the instrument automatically truncated the maximum load to a safe value.

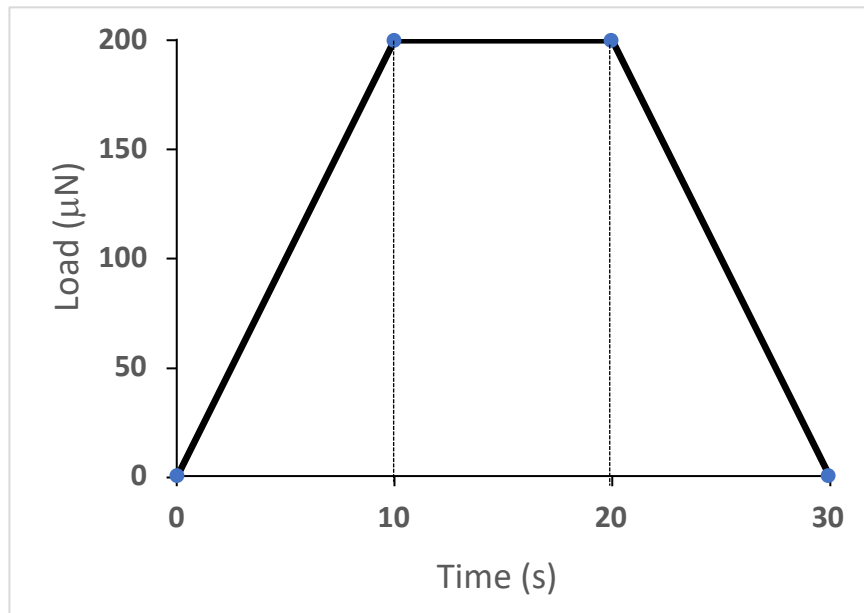


**Fig. 1: Loading profile**

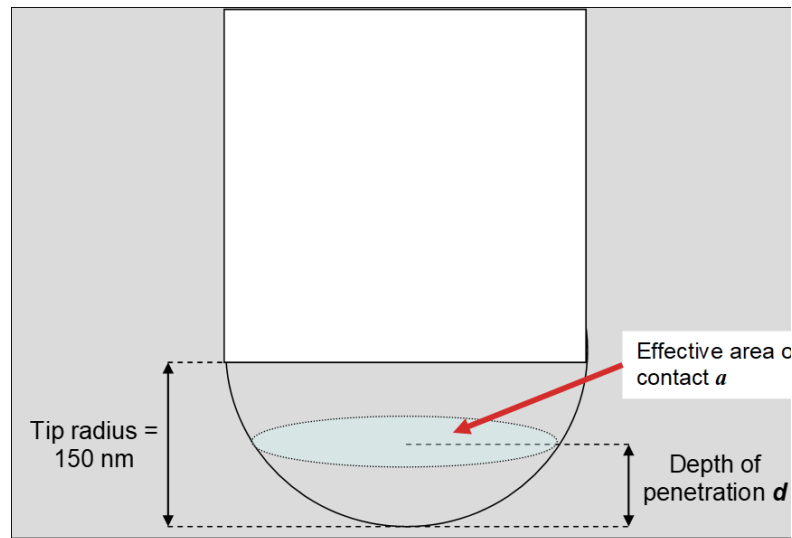


Fig. 2: Profile of indenter tip

A diamond hemispherical tip was used to bridge pores on the surface (Fig. 2). The radius of the nanoindenter tip was **150 nm**. This value was used to calculate the effective area of contact *a*. If the penetration depth is *d*, the effective area of contact is given as:  
 $a = \pi \cdot d \cdot (2 \times 150 - d) \text{ nm}^2$ , upto a depth of 150nm  
 $= \pi \times (150^2) \text{ nm}^2$ , when depth > 150nm  
 The stiffness was measured as the slope of the first 10% readings of the unloading curve. The hardness was

measured as the peak load divided by projected area. The reduced modulus was calculated using the following formula.

$$E_r = \frac{S\sqrt{\pi}}{2\sqrt{A}}$$

Where:  
 S is the stiffness and A is the projected area.

**Results and analysis**

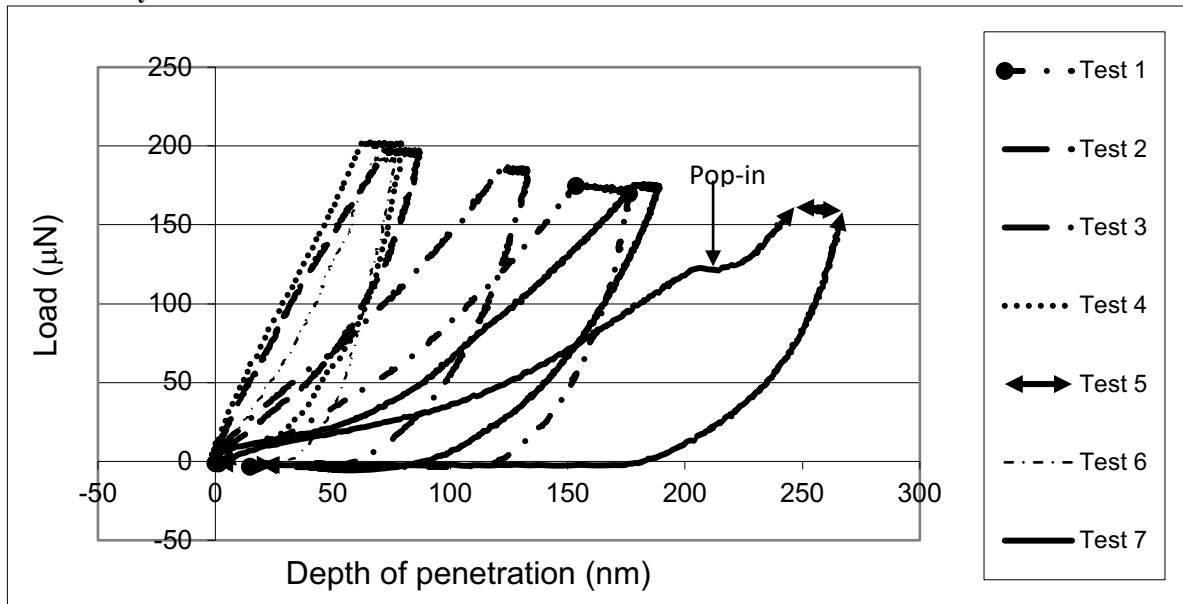


Fig. 3: Load-depth plots for cartilage

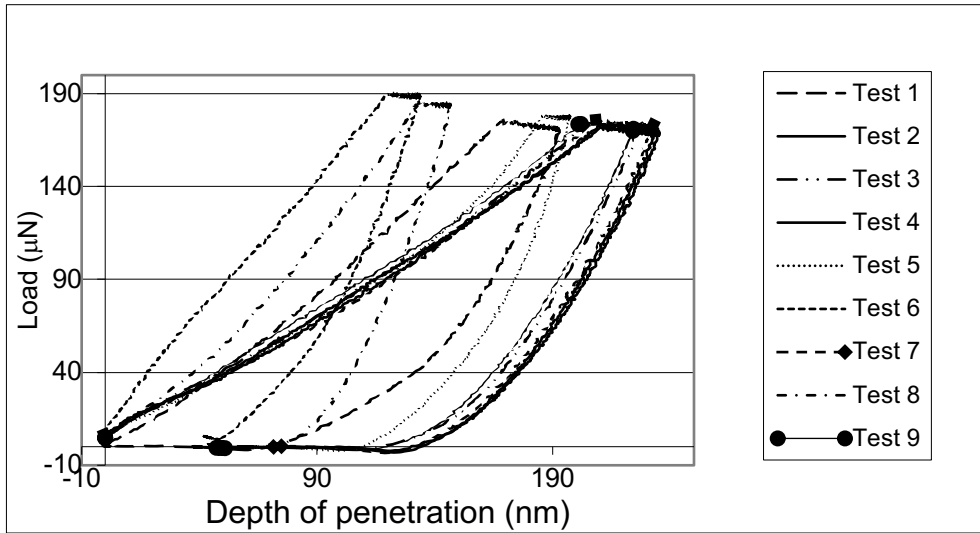


Fig. 4: Load-depth plots for PHN

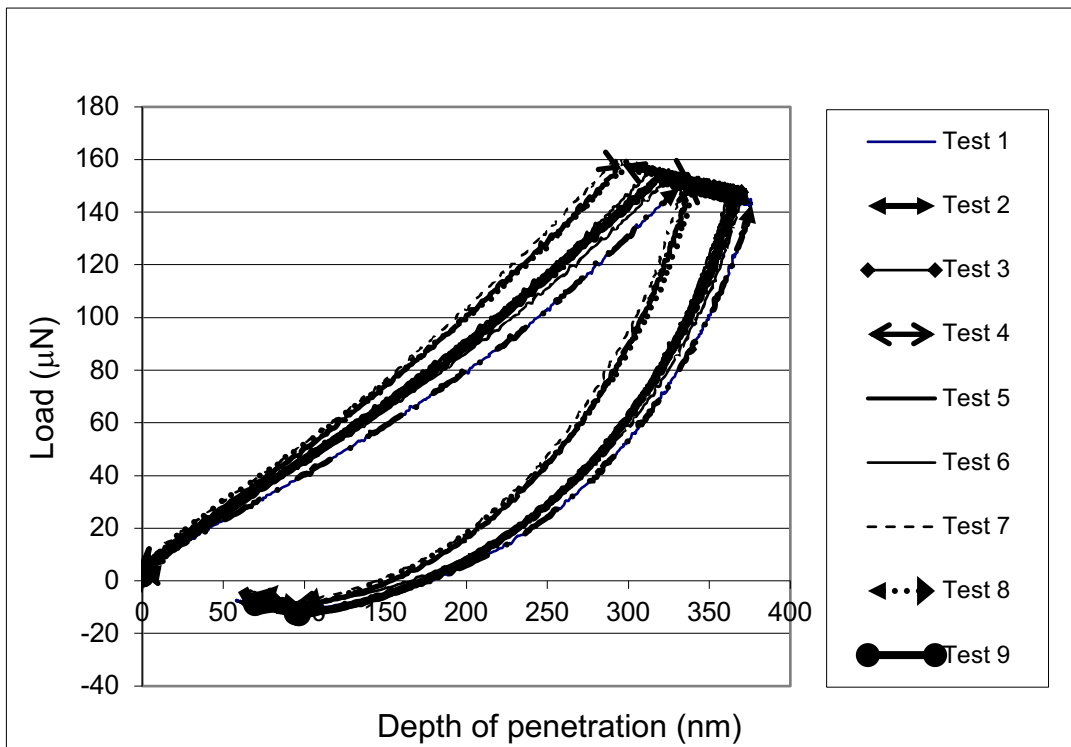
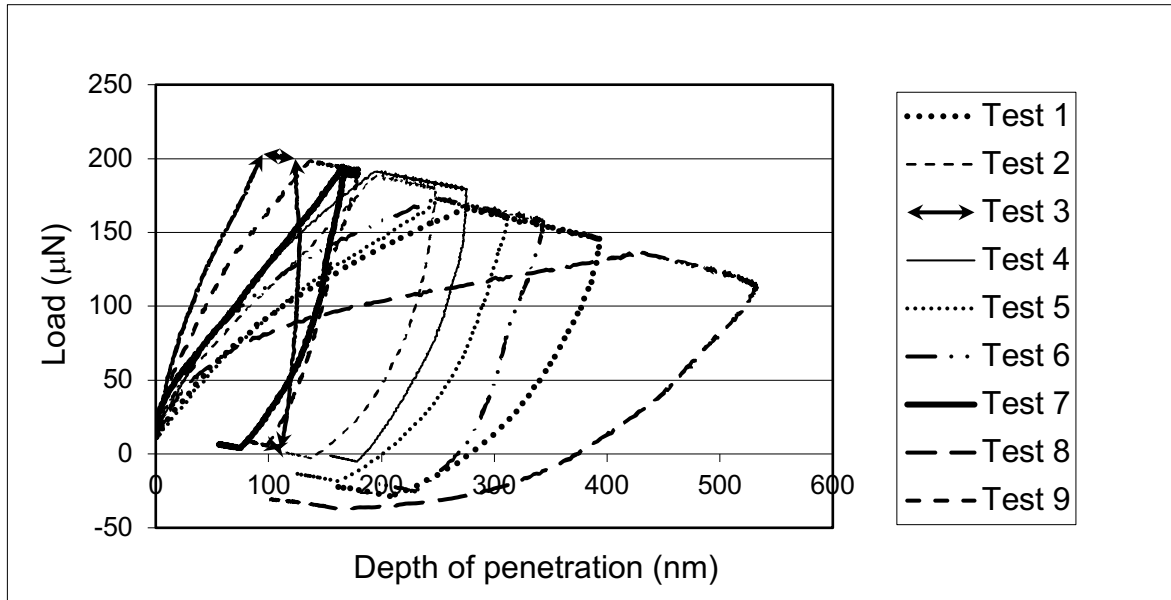


Fig. 5: Load-depth plots for UHMWPE



**Fig. 6: Load-depth plots for bone**

Figs. 3 to 6 show load-depth profiles for cartilage, PHN, UHMWPE and bone respectively. For cartilage, seven out of the nine test results are displayed, as the remaining two seemed to be erroneous. It has been found that it is very difficult to obtain meaningful and accurate nanoindentation data for viscoelastic biomaterials using quasi-static testing techniques due to surface size effects, indenter shape, force frequency and loading function.<sup>47</sup> There is large variation in the plots for cartilage and bone, the two naturally occurring composites (indicated by high values of standard

deviation). For PHN and UHMWPE there is less variation with UHMWPE being the most consistent. There is definitely creep deformation during the constant load period, for all tests of all materials with variations within each material and across materials. On reducing the load to zero, there is still finite deformation observed for all tests. Test number 5 for cartilage shows a pop-in kind of phenomenon [<sup>48,49,50</sup>] indicating a sudden failure at a certain load. This occurred for the test which exhibited maximum deformation.

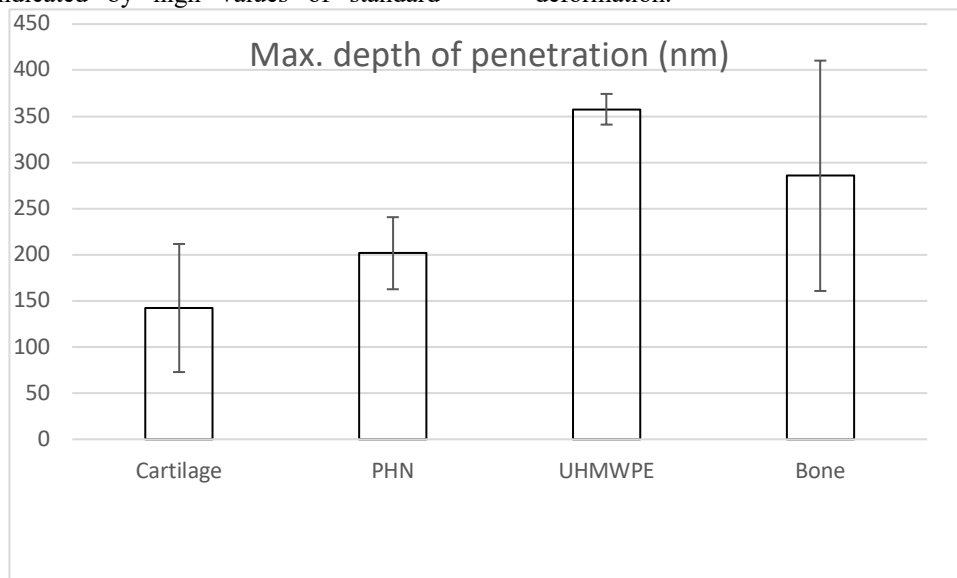


**Fig. 7: Maximum average penetration depth (with standard deviation bars)**

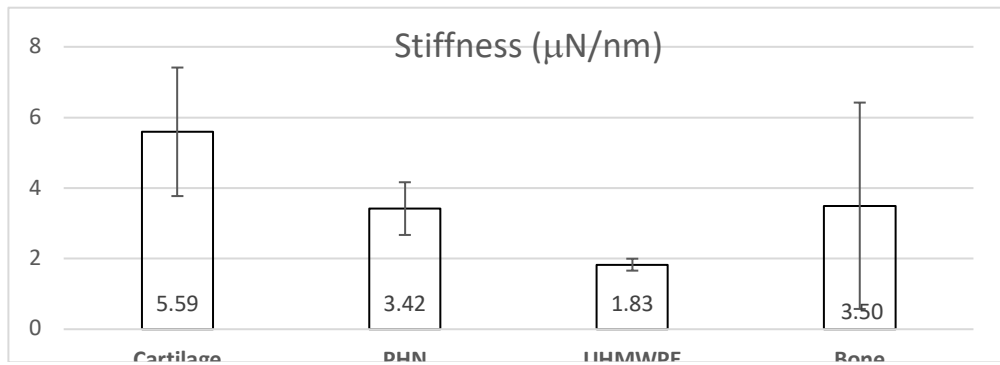


**Fig.8: Average stiffness (with standard deviation bars)**

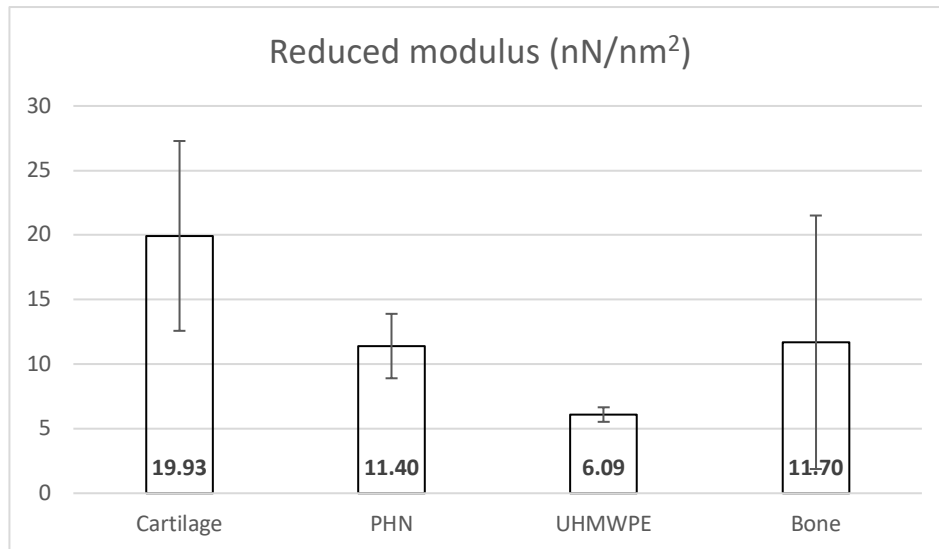


**Fig. 9: Average reduced modulus (with standard deviation bars)**

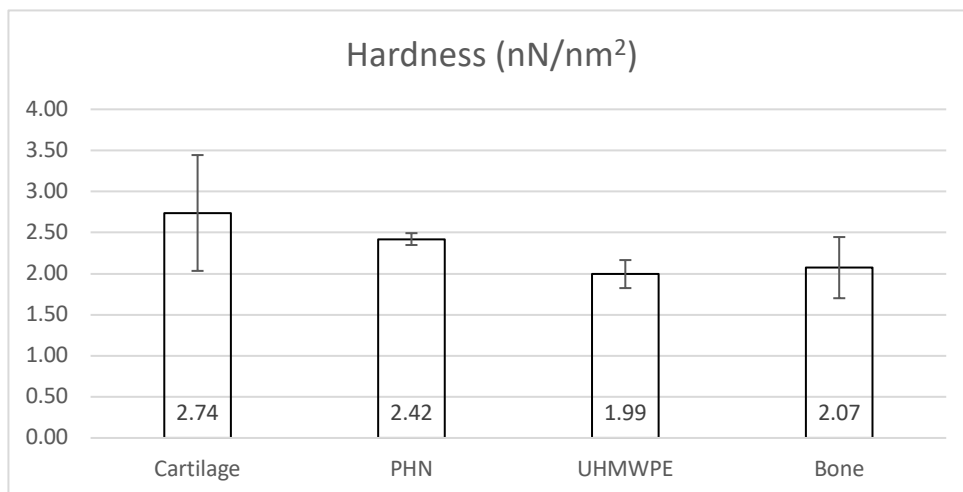


**Fig. 10: Average hardness (with standard deviation bars)**

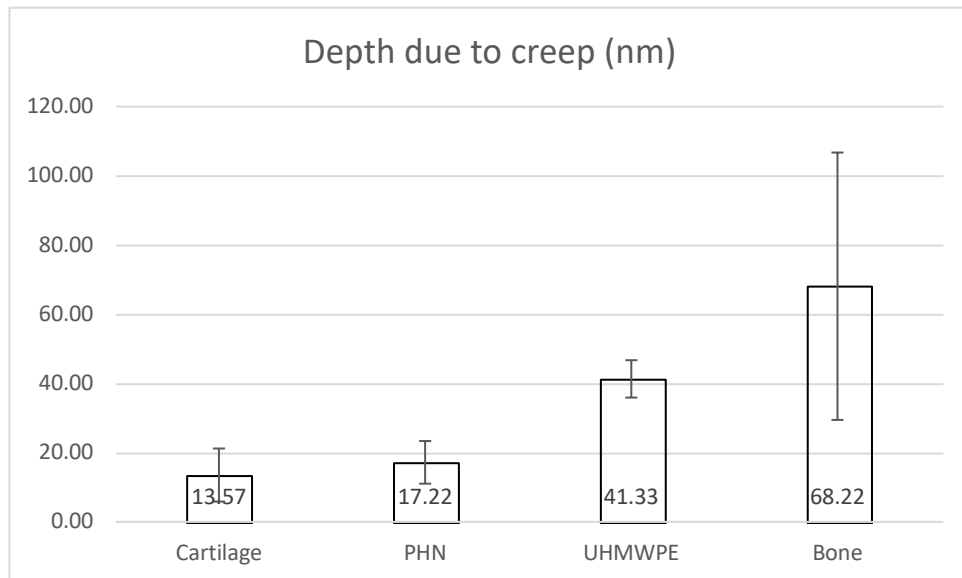


**Fig. 11: Depth due to creep (during constant load) along with standard deviation bars**

Cartilage and bone, in the dry state, exhibited the highest and second highest average stiffnesses and reduced moduli (Figs. 8 and 9). However, their standard deviations were much larger than those of the synthesized materials. This can be attributed to natural tissues being highly complex, anisotropic composite materials, with the surface varying from rigid fibers to empty pores [51]. The artificially synthesized materials, namely PHN and UHMWPE exhibited lower average stiffness and reduced modulus than that of dry cartilage and bone. However the values of PHN were close to that of bone. PHN showed a slightly larger average hardness value of hardness ( $2.42\text{nN/m}^2$ ) than that of bone ( $2.07\text{nN/m}^2$ ), but had a much lower standard deviation. UHMWPE had the lowest average stiffness, hardness and reduced modulus compared to the other materials, which corroborated with the highest depth of penetration.

An interesting observation was with the creep deformation. Bone exhibited the highest average value (68.22 nm) with the highest standard deviation. UHMWPE came up second with a much lower value of (41.33 nm). Third was PHN with a value of 17.22 nm and cartilage had a value of 13.57 nm. The standard deviation values of creep deformation for UHMWPE, PHN and cartilage were much lower than that of Bone. This indicates that bone, in the dry state, deforms to a very varied extent across the surface, under a constant load. On the other hand, cartilage in the dry state, had the lowest average creep deformation and much lower standard deviation than that of bone, exhibiting a stark contrast in creep behavior between the two natural materials. This could be attributed to cartilage being in a much collapsed state in the dry condition, with not much allowable deformation.

It is seen that the average values for PHN, along with the standard deviation, overlap those of cartilage tissue, indicating that the PHN composite can be tailored to mimic the behaviour of cartilage, thereby reducing stress shielding and possibly providing deformation leading to elastohydrodynamic lubrication. This is

evident from the friction results reported by Ribeiro et al in reference [3]. Mimicking bone would be a bigger challenge, due to the large variance in values.

### Conclusions

Cartilage, in dry state, exhibited the highest stiffness, hardness and reduced modulus which corroborated with minimum depth of penetration. This could be attributed to the high fiber concentration at the surface. On the other hand, UHMWPE exhibited the minimum stiffness, hardness and reduced modulus, corroborating with maximum depth of penetration. Bone exhibited the second highest stiffness and reduced modulus. However, its hardness was the third highest. The two natural tissues, namely cartilage and bone exhibited much higher standard deviation of properties owing to the complex nature of the tissues. PHN could be tailored to match the properties of cartilage and bone by varying its constituents. The results also indicate that PTMC as a drug delivery agent or sutures could be well tolerated by the body due to its tissue-like behavior.

### Acknowledgement

The author would like to thank Dr. H. Liang, Dr. D. Darensbourg, Dr. P. Ganguly and the Materials Characterization Facility of Texas A&M University for their support in this study. The author would also like to thank the US National Science Foundation (0535578) for their kind financial support.

### References

1. R. Ribeiro, Z. Shan, A.M. Minor, H. Liang, In situ observation of nano-abrasive wear, *Wear* 263, 1556-1569, 2007.
2. D. Huitink, L. Peng, R. Ribeiro, H. Liang, In situ observation of stress-induced Au-Si phase transformation, *Applied Physics, Letters* 94, 183111, 2009.

3. R. Ribeiro, P. Ganguly, D. Darensbourg, M Usta, A.K. Ucisik, H. Liang, Biomimetic study of a polymeric composite material for joint repair application, *Journal of Materials Research* 22(6), 1632-1639, 2007.
4. Dichu Xu, Terence Harvey, Eider Begiristain, Cristina Dominguez, Laura Sánchez-Abella, Martin Browne, Richard B. Cook, Measuring the elastic modulus of soft biomaterials using nanoindentation, *Journal of the mechanical behavior of biomedical materials*, 133, 105329, 2022.
5. A.C. Fischer-Cripps, Nanoindentation, Springer-Verlag, Berlin, Germany, 2022.
6. Tsui, T.Y., Pharr, G.M. Substrate effects on nanoindentation mechanical property measurement of soft films on hard substrates. *Journal of Materials Research* 14, 292–301 (1999). <https://doi.org/10.1557/JMR.1999.0042>
7. W.C. Oliver, G.M. Pharr, An improved technique for determining hardness and elastic modulus using load and displacement sensing indentation experiments. *Journal of Materials Research* 7, 1564–1583 (1992). <https://doi.org/10.1557/JMR.1992.1564>
8. M. Islam, M. Oyen, A poroelastic master curve for time-dependent and multiscale mechanics of hydrogels. *Journal of Materials Research* 36, 2582–2590 (2021). <https://doi.org/10.1557/s43578-020-00090-5>
9. M.V. Swain, J. Nohava, P. Eberwein, A simple basis for determination of the modulus and hydraulic conductivity of human ocular surface using nanoindentation, *Acta Biomaterialia* (50), 312-321. 2017.
10. D.M. Ebenstein, L.A. Pruitt, Nanoindentation of biological materials, *Nanotoday* 1(3), 26-33, 2006.
11. August 2006, Pages 26-33.
12. E.M. Hasler, W. Herzog, J.Z. Wu, W. Müller, U. Wyss, Articular cartilage biomechanics: theoretical models, material properties, and biosynthetic response, *Critical Reviews in Biomedical Engineering*, 27(6), 415-488, 1999.
13. Y.P. Zheng, A.F.T. Mak, A.K.L. Leung, State-of-the-art methods for geometric and biomechanical assessments of residual limbs : a review, *Journal of rehabilitation research and development*, 38(5), 487-504, 2001.
14. D. Tabor, The hardness of metals, Clarendon Press, London, UK, 1951.
15. J.H. Kinney, S.J. Marshall, G.W. Marshall, The mechanical properties of human dentin: A critical review and re-evaluation of the dental literature, *Critical Reviews in Oral Biology & Medicine*, 14(1), 13-29, 2003.
16. N.E. Waters, Some mechanical and physical properties of teeth, *Symposia of the society for experimental biology*, 34, 99-135, 1980.
17. J-Y Rho, T.Y. Tsui, G.M. Pharr, Elastic properties of human cortical and trabecular lamellar bone measured by nanoindentation, *Biomaterials*, 18(20), 1325-1330, 1997.
18. D.M. Ebenstein, A. Kuo, J.J. Rodrigo, A.H. Reddi, M. Ries, L. Pruitt, A nanoindentation technique for functional evaluation of cartilage repair tissue. *Journal of Materials Research* 19(1), 273-281, 2004. <https://doi.org/10.1557/jmr.2004.19.1.273>
19. <https://globalranetwork.org/project/disease-info/>
20. R. Ribeiro, S. Ingole, M. Usta, C. Bindal, A.H. Ucisik, H. Liang, A tribological comparison, of pure and boronized chromium, *Journal of tribology*, 128(4), 895-897, 2006.
21. R. Ribeiro, S. Banda, Z. Ounaies, H. Ucisik, M. Usta, H. Liang, A tribological and biomimetic study of PI–CNT composites for cartilage replacement, 47, 649-658, 2012.
22. B.L. Seal, T.C. Otero, A. Panitch, Polymeric biomaterials for tissue and organ regeneration, *Materials Science and Engineering: R: Reports*, 34, Issues 4–5, 147-230, 2001.
23. A.E. Beris, M. G. Lykissas, C.D. Papageorgiou, A.D. Georgoulis, *Advances in articular cartilage repair, Injury*, 36(4), Supplement, S14-S23, 2005.
24. B.H. Thomas, J.C. Fryman, K. Liu, J. Mason, Hydrophilic–hydrophobic hydrogels for cartilage replacement, *Journal of the Mechanical Behavior of Biomedical Materials*, 2(6), 588-595, 2009.
25. M. P. Nikolova, M.S. Chavali, Recent advances in biomaterials for 3D scaffolds: A review, *Bioactive Materials*, 4, 271-292, 2019.
26. R. Ma, D. Xiong, F. Miao, J. Zhang, Y. Peng, Novel PVP/PVA hydrogels for articular cartilage replacement, *Materials Science and Engineering: C*, 29(6), 1979-1983, 2009.
27. R. Ribeiro, M. Usta, A.H. Ucisik, H. Liang, Biomimetic study of a polymeric composite

- material for joint repair applications, *Journal of Materials Research*, 22(6), 1632-1639.
28. B.R. Rawal, R. Ribeiro, Biomaterials for cartilage repair, a review, *Journal of Medical Sciences*, 13(8), 615-620, 2013.
  29. B.J. Briscoe, L. Fiori, E. Pellilo, Nano-indentation of polymeric surfaces, *Journal of Physics D: Applied Physics*, 31(19), 1998.
  30. C. Klapperich, K. Komvopoulos, L. Pruitt, Nanomechanical Properties of Polymers Determined From Nanoindentation Experiments, *Journal of tribology*, 123(3), 624-631, 2001.
  31. L.A. Cyster, D.M. Grant, S.M. Howdle, F.R.A.J. Rose, D.J. Irvine, D. Freeman, C.A. Scotchford, and K.M. Shakesheff: The influence of dispersant concentration on the pore morphology of hydroxyapatite ceramics for bone tissue engineering. *Biomaterials* 26, 697, 2005.
  32. P. Ducheyne, Q. Qiu, Bioactive ceramics: The effect of surface reactivity on bone formation and bone cell function, *Biomaterials* 20, 2287, 1999.
  33. C. Klein, A.A. Driessen, K. de Groot, A. Vandenhooff, Biodegradation behavior of various calcium-phosphate materials in bone tissue. *Journal of biomedical materials research*, 17, 769, 1983.
  34. S.L. I-Riley, L.E. Okun, G. Prado, M.A. Applegate, A. Ratcliffe, Human articular chondrocyte adhesion and proliferation on synthetic biodegradable polymer films. *Biomaterials*, 20, 2245, 1999.
  35. A.R. Katz, D.P. Mukherjee, A.L. Kaganov, S. Gordon, A new synthetic monofilament absorbable suture made from polytrimethylene carbonate, *Surgery, Gynecology & Obstetrics*, 161, 213, 1985.
  36. R.A. Jain: The manufacturing techniques of various drug loaded biodegradable poly(lactide-co-glycolide) (PLGA) devices. *Biomaterials*, 21(23), 2475-2490, 2000.
  37. R.C. Edwards, K.D. Kiely, B.L. Eppley, The fate of resorbable poly-L-lactic/polyglycolic acid (Lactosorb) bone fixation devices in orthognathic surgery, *Journal of oral and maxillofacial surgery*, 59(1), 19, 2001.
  38. B.L. Seal, T.C. Otero, A. Panitch, Review of polymeric biomaterials for tissue and organ regeneration. *Materials Science and Engineering: R: Reports*, 34(4-5), 147-230, 2001.
  40. S.K. Smart, A.I. Cassady, G.Q. Lu, D.J. Martin, The biocompatibility of carbon nanotubes, *Carbon* 44(6), 1034, 2006.
  41. E. Cenni, D. Granchi, C.R. Arciola, G. Ciapetti, L. Savarino, S. Stea, D. Cavedagna, A Di Leo, A Pizzoferrato, Adhesive protein expression on endothelial cells after contact in vitro with polyethylene terephthalate coated with pyrolytic carbon, *Biomaterials* 16(6), 1223-1227, 1995.
  42. L. Ma and G. Sines, Fatigue behavior of a pyrolytic carbon, *Journal of Biomedical Materials Research*, 51A(1), 61-68, 2000.
  43. A.D. Haubold, Blood/carbon interactions. *ASAIO J.* 6, 88, 1983.
  44. C.A.V. Blitterswijk, J.J. Grote, W. Kuijpers, W.T. Daems, K.A. de Groot, Macropore tissue ingrowth: A quantitative and qualitative study on hydroxyapatite ceramic. *Biomaterials* 7(2), 137-143, 1986.
  45. T. Furuzono, P-L. Wang, A. Korematsu, K. Miyazaki, M. O-Mori, Y. Kowashi, K. Ohura, J. Tanaka, and A. Kishida, Physical and biological evaluations of sintered hydroxyapatite/siliconecomposite with covalent bonding for a percutaneous implant material. *Journal of Biomedical Materials Research Part B: Applied Biomaterials*, 65(2), 217-226, 2003.
  46. Bharat Bhushan, Biomimetics: lessons from nature – an overview, *Philosophical Transactions of the Royal Society A, Math Phys Eng Sci* 367 (1893): 1445–1486, 2009.
  47. D.J. Darensbourg, P. Ganguly, D.R. Billodeaux, Ring opening polymerization of Trimethylene carbonate using aluminum (III) and Tin (IV) salen chloride catalysts. *Macromolecules* 38(13), 5406-5410, 2005.
  48. D.H. Collins and G. Meachim, Sulphate (35SO4) fixation by human articular cartilage compared in the knee and shoulder joints, *Annals of the Rheumatic Diseases*, 20(2), 117-122, 1961.
  49. Zhang Y F, Bai S L, Li X K, Zhang Z. Viscoelastic properties of nanosilica- filled epoxy composites investigated by dynamic nanoindentation. *Journal of Polymer Science B: Polymer Physics*, 47, 1030–1038, 2009.
  50. Christopher A. Scuch, Nanoindentation studies of materials, *Materials Today*, 9(5), 32-40, 2006.
  51. D.A. Lucca, K.Herrmann, M.J. Klopstein, Nanoindentation: Measuring methods and

- applications, *CIRP Annals - Manufacturing Technology* 59, 803–819, 2010.
52. Zaid H. Mahmoud, H.N.K. Al-Salman, Ehsan Kianfar, Nanoindentation: Introduction and applications of a non-destructive analysis, *Nano TransMed*, 3, 100057, 2024
  53. Qiang Chen, Nicola M. Pugno, Bio-mimetic mechanisms of natural hierarchical materials: A review, *Journal of the mechanical behavior of biomedical materials*, 19, 3-33, 2013.